

Review

Focus on Materials for Sulfur-Resistant Catalysts in the Reforming of Biofuels

Patrizia Frontera ^{1,2} , Pier Luigi Antonucci ³ and Anastasia Macario ^{4,*} 

- ¹ Civil Engineering, Energy, Environmental and Materials Department, University of Reggio Calabria, Via Salita Melissari, 89124 Reggio Calabria, Italy; patrizia.frontera@unirc.it
- ² Consorzio Interuniversitario per la Scienza e la Tecnologia dei Materiali—INSTM, Via Giuseppe Giusti, 9, 50121 Firenze, Italy
- ³ Istituto di Tecnologie Avanzate per l'Energia "Nicola Giordano", Consiglio Nazionale delle Ricerche, Via Salita Santa Lucia sopra Contesse, 5, 98126 Messina, Italy; pierluigi.antonucci@unirc.it
- ⁴ Environmental Engineering Department, University of Calabria, Via Pietro Bucci, 87036 Arcavacata di Rende, Italy
- * Correspondence: macario@unical.it; Tel.: +39-0984-496-704

Abstract: The reforming of biofuels represents a promising technology for *low carbon* and *renewable hydrogen* production today. The core of the process is an active and stable catalyst, which can help to improve this technology and its efficiency. With this review, we aim to survey the more relevant literature on heterogeneous catalysts for the reforming of biofuels with improved sulfur tolerance. The review is structured into four main sections. Following the introduction, the fundamental aspects of sulfur poisoning are discussed. In the third section, the basic principles of the reforming of biofuels are reported, and finally, in the fourth section—the core of the review—recent progresses in the development of sulfur resistant catalysts are discussed, distinguishing the role of the metal (noble and non-noble) from that of the support.



Citation: Frontera, P.; Antonucci, P.L.; Macario, A. Focus on Materials for Sulfur-Resistant Catalysts in the Reforming of Biofuels. *Catalysts* **2021**, *11*, 1029. <https://doi.org/10.3390/catal11091029>

Academic Editor: David Kubička

Received: 31 July 2021

Accepted: 23 August 2021

Published: 26 August 2021

Publisher's Note: MDPI stays neutral with regard to jurisdictional claims in published maps and institutional affiliations.



Copyright: © 2021 by the authors. Licensee MDPI, Basel, Switzerland. This article is an open access article distributed under the terms and conditions of the Creative Commons Attribution (CC BY) license (<https://creativecommons.org/licenses/by/4.0/>).

Keywords: sulfur; reforming; biofuels; carbon oxides; catalysts; decarbonization; renewable hydrogen; net-zero emission

1. Introduction

In order to contribute to decarbonization, today's energy sector is called to respond to a complex challenge: to simultaneously satisfy the recent energy needs of an increasingly large population, and to limit greenhouse gas emissions. On the one hand, there are promising solutions to supply the future energy demand, such as the recovery of waste energy and various technologies that produce power from renewable sources [1–4]. On the other hand, the last World Energy Outlook of the International Energy Agency explained what it means for the energy sector to achieve *net-zero emission* by 2050 (NZE2050) [5]. Several countries, in their national development policies, have introduced stringent goals to achieve *net-zero emission* by 2050. International actions that will be implemented in the next decade will have a decisive role in reaching the 2050 objective. First of all, CO₂ emissions should decrease by at least 45% from 2010 to 2030. This gives the energy and industrial sectors a 2030 target of 20.2 Gt CO₂ that must not be exceeded, as shown in Figure 1 [6].

The next COP26 will be a further milestone in the path aimed at achieving the objectives of the Paris Agreement, which aims to reduce the global temperature increase to 1.5 °C. In this scenario, the promotion of hydrogen use can make an important contribution to reduce emissions, and could represent a solution to the decarbonization of highly energy-intensive industrial sectors. Alternative energy sources to hydrogen production have been considered in order to promote the use of this energy vector. There are several production processes of traditional hydrogen or *low carbon hydrogen*: steam reforming of natural gas

or of oxygenated hydrocarbons, gasification, electrolysis of water, biological processes, etc. [7–13]. Very recently, the Italian energy giant, ENI SpA, has published an interesting report—"Eni for 2020–Carbon Neutrality by 2050"—in which one of its strategies to reach this important milestone is to intensify hydrogen production using different technological paths: reforming of natural gas combined with the CO₂ capture (called *blue hydrogen*), catalytic partial oxidation of natural gas or biomethane (*kGas technology*), gasification of non-recyclable waste (*waste-to-hydrogen*), and electrolysis of water by renewable energies (called *green hydrogen*) [14].

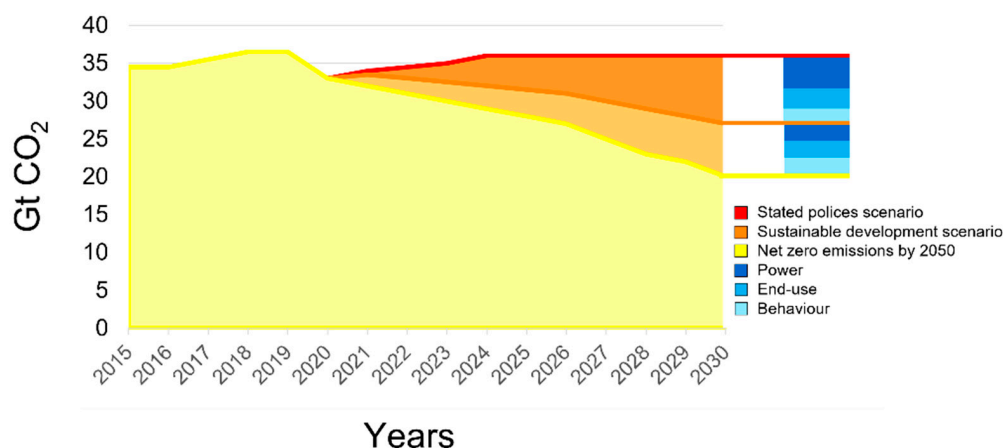


Figure 1. CO₂ emissions and forecasting of reduction levels (adapted from [6]).

Beyond these processes, due to the technological advancements in stationary energy systems—such as the fuel cells—reforming of biofuels is currently an interesting alternative for renewable hydrogen production [15–21]. Using biofuels to produce hydrogen means reducing net carbon dioxide emissions in energy production: hydrogen derived by biomass can be used in the solid oxide fuel cells (SOFCs) to the direct conversion of fuels into electricity [21,22]. Ethanol, glycerol, and biodiesel are the most promising candidates for hydrogen production due to their low toxicity and safety in handling, while the most efficient processes are the catalytic ones [23–25]. The most active species in these processes are noble metals and nickel-based catalysts, which are the typical catalysts for reforming reactions [26–31]. High carbon and sulfur poisoning resistance are required for these catalysts. It is well known, in fact, that the presence of heavy hydrocarbon and sulfur compounds can deteriorate the reforming catalyst.

To overcome these limitations, chemical modifications of support and metal active species have been applied to the catalyst synthesis procedure. High carbon deposition resistance can be achieved by catalysts containing alkaline earth metal oxides and rare earth oxides in the support [15,32–36].

Moreover, avoiding metal sintering particles is another aspect deeply investigated by researchers in order to reduce the coke deposition during the reforming reaction [37–40]. If the deactivation of the catalyst does not involve the metal particles sintering phenomenon, the spent catalyst by coke deposition can be recycled and reused after the appropriate re-activation procedures are able to remove carbon particles deposited on the catalyst surface [41].

The presence of Mo, Re, or Pd as additional active species is the main solution to improve the sulfur resistance of the catalyst [23,27,42–45].

Recently, Yeo et al. reviewed the various strategies that have been developed to impart sulfur resilience and improve reforming performance where sulfur compounds are considered as valuable reactants in order to look at some possible directions moving forward [46].

The aim of this review is to point out, discuss, and highlight the main features of catalytic materials that are resistant to sulfur poisoning for the reforming of biofuels. The

catalyst sulfur resistance is always strongly dependent on the materials of both the active metal species and the support used in the design of the catalysts. After the fundamentals of reforming reactions and the formation of sulfur compounds are discussed, the review will deal with the role of materials on the development of reforming catalysts resistant to sulfur poisoning, in hopes of giving the reader a useful tool through which more promising results can be achieved.

2. Fundamentals on Sulfur Poisoning

The loss of activity and/or selectivity of most transition metals can occur for several reasons in the catalytic process, such as a temperature that is too high, or a steam/hydrocarbon ratio that is too low. These wrong conditions can cause coke deposition on the catalyst surface in a very short time of reaction. At the same time, several reactants' contaminants that are present in the feed can completely deactivate the reforming catalyst: it is well known that sulfur can be one of these. In a hydrocarbon feed, sulfur can be present in organic or inorganic form. The most common inorganic sulfur compound is hydrogen sulfide (H_2S), while the organic ones are carbon disulfide (CS_2), carbonyl sulfide (COS), dimethyl sulfide (DMS), and thiophene ($\text{C}_4\text{H}_4\text{S}$).

In fuels derived from natural sources, the concentration of sulfur species can be included within a very wide range. For example, the sulfur level in biodiesel is present as trace, and in amounts lower than 10 mg/Kg [47,48], while the sulfur level in biogas—mainly present as H_2S —is 1500 ppm_v on average [49,50].

Without any pre-treatment, these biofuels can poison the reforming catalyst. Only 10 ppm of H_2S can deactivate the nickel catalyst, although temperature, reaction time, and catalyst geometry strongly affect the catalyst stability [51]. The main cause of catalyst deactivation is the irreversible chemisorption of the sulfur on catalytic active sites. The poisoning effect of sulfur is due to its high adsorption strength, with respect to that of other species that are competing for catalytic sites in the reaction media.

Many of the studies that deal with the poisoning effect of sulfur have been carried out on nickel-based catalysts, but the mechanism by which sulfur affects the catalyst surface can be generalized independently of the metal.

First of all, the mechanism through which sulfur can irreversibly affect the activity of the catalyst starts by a physical blocking of one or more adsorption and reaction sites. Second, due to its strong chemical bond, sulfur modifies the nearest neighbor of metal atoms electronically (Figure 2). This consequently and irreversibly modifies the ability of these metal atoms to adsorb or dissociate other reactants' molecules [52]. It has been evaluated that these effects can extend up to about 5 a.u. [53].

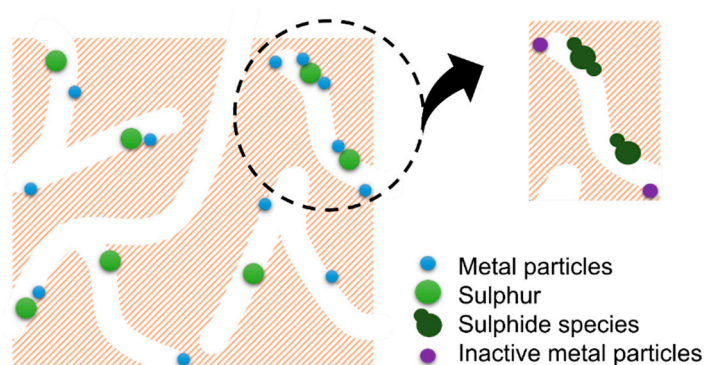


Figure 2. Schematization of the poisoning effect of sulfur on catalysts.

Several works have studied the structure of sulfur adsorbed on Ni metal, and indicated that sulfur adsorbed on nickel catalysts is more stable than sulfide species present in the bulk (Ni_3S_2 , Ni_2S_3) [54–56]. Some of these authors have reported that the saturation coverage of sulfur on Ni(100) occurs more easily than on that of Ni(110) or Ni(111). For

example, for Ni(110), the saturation coverage occurs at $S/Ni_s = 0.5$, while a higher S/Ni_s ratio is necessary to achieve the saturation coverage for more open surface structures, such as Ni(110) [55,56]. Since the sulfur adsorption on a metal surface is very strong, its poisoning effect on the other transition metals, such as Fe or Ru, is considered similar, even if there are no studies on the other transition metals so thorough as those relating to sulfur/nickel [57].

From a chemical point of view, since the reactivity of sulfur depends on the number of electron pairs available for bonding, the H_2S is more dangerous for metals than the SO_2 or SO_2^- species [52].

Recently, Beale et al. showed an interesting chemical imaging of the sulfur-induced deactivated Cu/Zn/ Al_2O_3 industrial catalyst in the WGS reaction [58]. They observed that H_2S concentration has a significant effect on catalyst activity due to the formation of crystalline sulfur-containing phases, including CuS, Cu_2S , $CuSO_4$, and β -ZnS. Moreover, sulfur-containing species also show different spatial distributions, revealing that Cu_2S and $CuSO_4$ species are mainly present in the edge of the sample, named *egg-shell like*, while CuS and β -ZnS species are mainly present in the sample periphery—described as *egg-white*—but not in the shell. Finally, no sulfur-containing species are present in the center of the sample, known as the *egg-yolk* region (Figure 3). They concluded that the Cu/Zn sulfides species formed at the shell of the catalyst destroy the catalyst porosity, avoiding the diffusion of other molecules inside the catalyst structure and preventing further sulfides species formation [58].

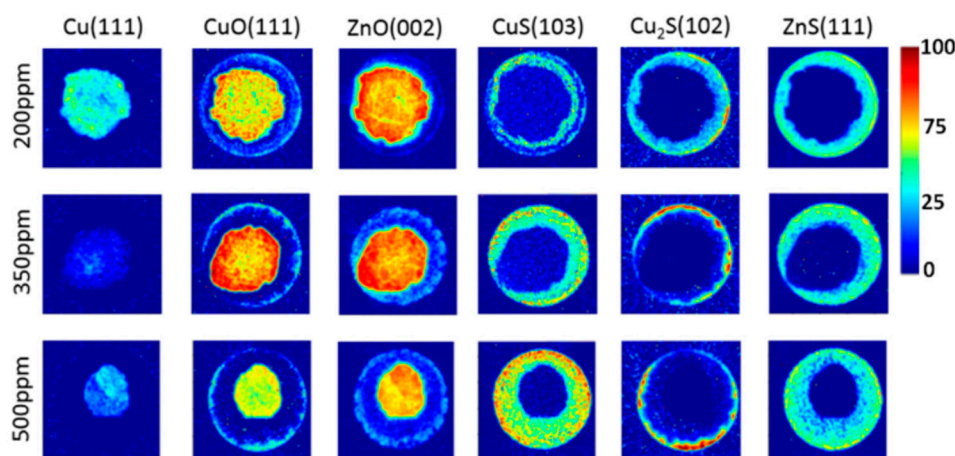


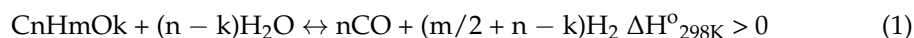
Figure 3. XRD intensity color maps showing different spatial distributions of sulfur-containing species. The analyzed sample is a microtomed cross section of a catalyst pellet (100 μm thick). On the right-hand side is a thermal scale bar. Reprinted with permission from [58].

The poisoning due to sulfur compounds is remarkable also in the CH_4 oxidation [59] and in the diesel oxidation reactions [60] in the presence of novel metals Pt/Pd bimetallic catalysts. However, further SO_2 oxidation studies on Pd/Pt mono- and bimetallic Al_2O_3 supported catalysts reveal that the catalysts with a higher Pt content were more active in terms of apparent SO_2 to SO_3 oxidation, based on outlet gas-phase measurements. Diffuse reflectance infrared Fourier transform spectroscopy (DRIFTS) studies showed indeed that higher Pd content catalysts were more active for oxidizing surface sulfur species at low temperatures. Moreover, in an oxygen atmosphere, Pd uptakes less SO_2 than Pt, but inhibiting species, such as palladium sulfates, are stabilized on the catalyst surface at higher temperatures [61]. These observations on the behavior of noble metals can be extended to the catalyst for the reforming of biofuels in the presence of sulfur compounds.

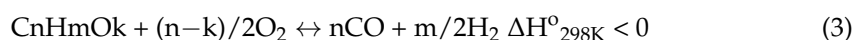
3. Reforming of Biofuels

The use of biofuels in reformation processes reveals several advantages derived from its renewable nature and potential integration in the process of H_2 production.

Today, the main process of H₂ production from generical hydrocarbon is steam reforming (SR) (Equation (1)) [15,62–64]:



The addition of oxygen to the reaction mixture provides a more advantageous energy balance within the process, owing to the use of exothermic heat of the oxidation reactions in Equations (2) and (3) for the energy supply of the endothermic reforming reaction in Equation (1):



The coupling reaction of Equation (1) with the reaction of Equation (2) or (3) allows the autothermal conditions to be obtained, generating a global process called autothermal reforming (ATR).

Also, the dry reforming (DR) of hydrocarbon fuels indicated in Equation (4) has received considerable attention for H₂ production due to the utilization of greenhouse gas –CO₂ [63,65–67]:



Hydrogen is considered to be a clean and effective energy carrier. Therefore, other processes for its production must be envisaged due to the environmental problems derived from the use of fossil feedstocks, so that the use of biofuels can contribute to this finality.

Generally speaking, biofuels are any renewable combustible fuels derived from recent (non-fossil) living matter, and include solid, liquid, or gaseous fuels derived from biomass.

The term “solid biofuel” is attributed to materials like wood, sawdust, leaves, and to all other forms of waste or renewable biological matter used as fuel. Steam reforming of solid biofuels is also known as steam pyrolysis or steam gasification, where an oxidizing agent such as oxygen or air is provided so that it approaches an autothermal process [68,69]. The ISO 16994:2016 describes methods for the determination of the total sulfur and total chlorine content in solid biofuels [70]. The content of sulfur depends on the origin of the solid biofuels (Figure 4). The sulfur concentration is usually low in woody biomass, and the damage of the sulfur content is related to the process of direct combustion, where the noticeable amounts of S_{ox}—depending obviously on the initial S content—may be produced.

Among liquid biofuels, bioethanol and biodiesel are the potential biofuels devoted to H₂ production through on-board reforming, in accordance with Demirbas [71], who concludes through a deep analysis that bioethanol and biodiesel are the liquid transportation fuels with the highest potential to replace gasoline and diesel fuel in the future [71].

Currently, bioethanol, which is mainly derived from the fermentation of sugar cane and starch, is by far the most widespread non-fossil alternative fuel in the world. Actually, the world production of bioethanol increased from 24.5 million metric tons in the year 2004 to 110 million metric tons in 2019 [72].

Biodiesel is a fatty acid methyl ester (FAME) which is produced from the transesterification of vegetable oil with methanol. Glycerol emerges as a by-product, and can be further used for the food industry and pharmaceutical applications. The world production of biodiesel increased from 2 million metric tons in the year 2004 to 41 million metric tons in 2019 [79].

Sulfur content (wt%) of BIOFUELS

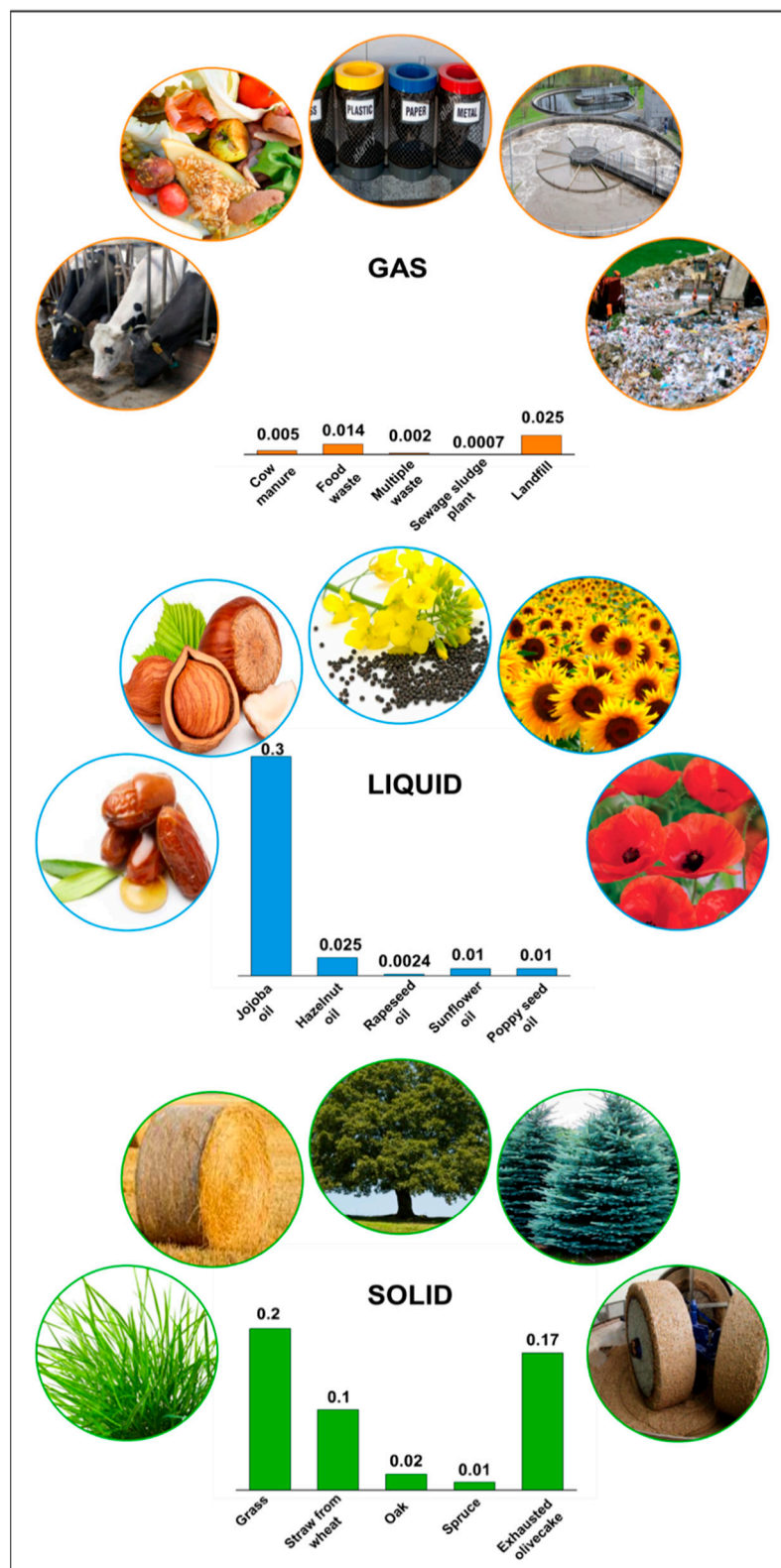


Figure 4. A few examples of sulfur content (wt%) in solid [73,74], liquid [75,76], and gaseous [77,78] biofuels.

The main challenge related to biofuel reforming is to avoid the deposition of coke on the catalyst surface, resulting in performance losses. Furthermore, catalyst deactivation can be caused by sintering and/or sulfur poisoning [80].

The properties of bioethanol depend strongly on its purity. In particular, the impurity of sulfur plays a significant role [81]. The content of sulfur in bioethanol depends also on raw sources, as shown in Figure 4.

Sulfur components have a more noxious effect on steam reforming than other impurities present in bioethanol. Yamazaki et al. [82] attributed the loss of the catalytic performance of Pt/ZrO₂ at 400 °C in the steam reforming of corn bioethanol to both sulfur compounds and the second generation of bioethanol, obtained by the fermentation of lignocellulosic biomass with a high content of sulfur compounds. Thus, a significant decrease of ethanol productivity is observed in steam reforming [21]. Extensive simulation performed by Martin et al. [19], including a variation of the reforming temperature, the air ratio, and the steam-to-carbon ratio highlighted that the reforming of bioethanol and biodiesel is a suitable perspective in sustainable clean energy production because of its lower system complexity and better dynamic behavior [19].

Biodiesel is one of the oxygenated hydrocarbon candidates of fuel for internal reforming solid oxide fuel cells (SOFCs) [83,84]. Generally, biodiesel contains less sulfur than fossil diesel; however, its composition depends on its raw feedstock and suppliers (Figure 4). For instance, the biodiesel derived from soybean oil (SO) contains several ppm of sulfur compounds, which is highly dependent on the crop conditions (e.g., soil properties and fertilizers) and region [85]. On the contrary, considering scum holds as a biodiesel feedstock, the sulfur content ranges from 600 to 1000 ppm [86]. Limits to the sulfur content in biodiesel have been restricted by some governments and agencies across the world. According to EN 14214 in Europe, the maximum allowable amount of sulfur in biodiesel is 10 mg kg⁻¹, compared with that of 500 mg kg⁻¹ according to ASTM D6751 in the United States [87,88].

However, the main challenge in biodiesel reforming studies is its multi-compound and variable composition, as well as the quantity of unsaturated esters [20] that affect the catalyst performances [89–91].

Among biofuels, biogas is more suitable for H₂ production via reforming, as attested by the exponential increase in articles on syngas production from biogas reforming [92]. Biogas contains CH₄ and CO₂ as main components, as well as N₂, O₂, H₂O, and trace amounts of other gases (e.g., H₂S, NH₃, and H₂). If its composition is affected by the type of feedstocks/waste sources utilized [93,94], then the sulfur content is variable, as shown in Figure 4.

Natural gas and biogas are essentially the same type of gas: methane. However, there are significant differences in the characteristics of biogas and natural gas. Natural gas is mainly composed of methane (95%) and ethane (5%), whereas biogas mainly contains methane (45–65%) and carbon dioxide (30–40%). The higher content of carbon dioxide (30–40%) determines the much lower energy of biogas as compared to natural gas [95]; however, an indisputable advantage of biogas with respect to natural gas is its renewability without the addition of any GHGs (Greenhouse Gases) to the atmosphere. Moreover, it helps in reducing the pollution produced by organic wastes, and mitigates waste management disposal [96].

4. Materials for Catalytic Sulfur Resistant Systems

The catalytic systems for the reforming of biofuel poisoned by sulfur compounds are continuously under investigation, as evidenced by the representative varying research reported in Table 1, and as referred to over the last two years. In the research, the main points that are investigated are the active metallic phase, which is in most cases nickel-based, and a second metallic phase supported on different materials. In the following sub-paragraphs, the identification of materials employed in the aforementioned main points of investigation are reported.

Table 1. Representative recent trends (last two years) on the catalyst interactions of the reforming of biofuels with sulfur compounds.

Catalysts	Process Involved	References
Commercial Ni catalyst	Methane trireforming in the presence of 1000 ppm H ₂ S and SO ₂ (± 19 ppm)	[97]
Ni/Al ₂ O ₃	Tar reforming (Naphthalene was used as the representative tar compound, with a content of 50 ppmv H ₂ S)	[98]
Ni/CeO ₂ -ZrO ₂	Dry reforming of methane (DRM) with two different amounts of feed sulfur: <1 ppm and 20–30 ppm	[99]
Mo/Ni-CeO ₂	Anodic catalyst in a direct internal reforming solid oxide fuel cell (DIR-SOFC), fed by biogas containing sulfur and siloxanes simultaneously	[100]
Ni/coal fly ash	Glycerol steam reforming (sulfur is due to support catalyst)	[101]
Rh(1%)/MgAl ₂ O ₄ /Al ₂ O ₃	Steam reforming of a synthetic biogas stream containing 200 ppm of H ₂ S, carried out in a membrane reactor	[102]
Ni-Rh/MgAl ₂ O ₄	Autothermal and steam reforming of methane in the presence of H ₂ S and NH ₃	[103]
M-CaO-Al ₂ O ₃ (M = Ni or Co)	Steam reforming of surrogate diesel (dodecane) with 100 ppmv of Thiophene	[104]
MoOx decorated Ni/SiO ₂ catalyst	Dry reforming of methane with 5000 ppm H ₂ S	[105]

4.1. Role of Metal Phases

4.1.1. Non-Noble Metals

The large number of papers regarding the use of nickel as a catalyst for reforming processes is related to the ability of this metal to break C–C bonds and promote water-gas shift reactions, thus increasing hydrogen production. The interest of researchers on Ni-based catalysts is due to their lower cost and higher availability as compared to noble metal catalysts, as well as their considerable intrinsic activity, especially when the metal is highly dispersed over a support [106]. However, the use of nickel-based catalysts has presented a significant challenge due to active metal sintering and coke deposition, which leads to catalyst deactivation, and, consequently, poor stability [107–110].

The deactivation of Ni-based catalysts due to S poisoning has also been the focus of many studies [111,112] in the field of SOFCs. The chemical compound with major negative effects is hydrogen sulfide, which reacts with nickel, the main anodic constituent, forming sulfides and blocking catalytic sites for electrode reactions. Furthermore, hydrogen sulfide interacts with all cell components via physical, chemical, and electrochemical mechanisms [113]. Among the fuel cells, molten carbonate fuel cells (MCFC) are particularly suitable for bioenergy production because they can be directly fed with biogas, which can then be transformed to hydrogen through internal reforming. However, the use of biogas containing hydrogen sulfide as MCFC fuel causes anode degradation and, consequently, the decay of cell performances, such as power output and durability [114–117].

The addition of a secondary metal to the metallic phase can have a positive effect on the resistance to sulfur poisoning, as a result of electronic perturbations produced by metal–metal bonding, or as a consequence of changes in the number of active sites present on the surface [118].

Cobalt is more resistant to sulfurization in comparison with nickel [99,119]. The combination of these metals produces a synergistic effect of bimetallic anode and the biodiesel feed, at a concentration of 5% hydrogen sulfide. An exchange current density of 1.91 mA/cm² and significant fuel cell life has been observed by [120].

In the dry reforming of biogas, a bimetallic catalyst in which cobalt was impregnated before nickel resulted in the development of active, stable, non-precious metal catalysts, in

which the cobalt acts as a sacrificial element to improve the sulfur tolerance of the nickel species [121].

Molybdenum also appears to have certain supportive properties against sulfur deactivation when combined with nickel. In the dry reforming of biogas, Gaillard et al. [122] found that while monometallic molybdenum and nickel catalysts are prone to deactivation, the Ni-doped Mo-based catalysts exhibit enhanced stability in the presence of sulfur in the feed [122]. Quincoces et al. [123] found for the CO₂ reforming of H₂S-odorized methane that a small amount of Mo exhibits an important thioresistance, independently of the impregnation sequence [123].

4.1.2. Noble Metals

Improved sulfur tolerance combined with a resistance to coke deactivation is claimed for precious metal catalysts such as Rh, Pt, Pd, and Au [118].

Rh has shown a high resistance to sulfur poisoning, yielding high conversion of hydrocarbons and high selectivity for H₂ [124–126]. A precious metal catalyst with an overall Rh loading of 69.1 g/ft³ onto a monolith support has been investigated in biodiesel steam reforming at various operating conditions, including a variation of temperature, pressure, steam-to-carbon ratio, and gas hourly space velocity. The biodiesel produced by the transesterification of soybean oil (40%) and palm oil (60%) with a low content of sulfur was used as a feedstock for steam reforming experiments, revealing that the precious metal catalyst improved performance over the ceramic-based catalyst at similar conditions [127].

Xie et al. [128] demonstrated that the Rh catalyst possesses a stronger capability to maintain carbon gasification activity in the reforming of liquid hydrocarbons than a Ni catalyst in the presence of sulfur.

The high sulfur resistance of the bimetallic Rh-Ni alumina catalyst is related to the spillover effect of sulfur from rhodium to the Ni-Rh phase separation surface. The protection effect of nickel is due to the reaction of this metal with sulfur adsorbed on rhodium [6].

Small amounts (0.1%) of palladium or platinum added to nickel catalysts for the reforming of methane demonstrated the greatest resistance to the action of H₂S (3500 ppm). The resistance of the catalysts to the poisoning by H₂S increases in a sequence that coincides with an order of the corrosion resistance of metal active components of composites in the air saturated with water vapor, containing a trace of hydrogen sulfide (Ni < Pt < Pd) [129].

An addition of Pd to Ni-based catalysts in the anode of a solid oxide fuel cell enhances the sulfur tolerance of Ni/GDC cermet (Gadolinium Doped Ceria), especially in the low H₂S concentration range (e.g., <100 ppm), indicating that the enhanced sulfur resistance of a Pd/Ni bimetallic catalyst is attributable to the promotion effect of impregnated Pd nanoparticles on the diffusion processes [130].

An addition of Au (2.3 wt%) to Ni-based catalysts allows it to obtain an enhanced sulfur tolerance in the steam reforming of methane in H₂S (10 ppm). The Au on the bimetallic catalyst promotes two effects: i) the hindering of the sulfur diffusion from the support surface to the catalytically active Ni sites, and ii) the production of an Au-Ni alloyed surface that inhibits the formation of strongly bonded sulfur compounds, such as Ni sulfide [131].

4.2. Materials for Catalyst Support

The support is an important element in the catalyst design, as it has the function of a skeletal framework that distributes the active metal particles. The interaction with the support is very important since it stabilizes the metal particles by modifying their electronics and morphological properties, and consequently affecting their reactivity [132,133]. In particular, the catalytic activity and/or selectivity may be improved as a result of the interactions with the support.

Alumina is the catalyst support largely used for its ability to disperse the supported phase, but also for its high thermal stability and availability. The capacity to disperse the metal phases is associated with its very stable surface OH groups, its Lewis acidity,

and the very high polarity of the surface acid–base pairs, which provide specific sites for anchoring cationic, anionic, and metallic species [134]. The catalyst traditionally used in steam reforming is based on nickel metal dispersed on alumina. The process operates at a high-temperature ($T = 700\text{--}900\text{ }^{\circ}\text{C}$) and at a space velocity between 3000 to 8000 h^{-1} [95,135]. However, alumina, due to its acidity, causes cracking of hydrocarbons, which is not desirable in fuel reforming as it may lead to deposits of coke on the catalytic surface, which is “inert” regarding the sulfur poisoning [111].

The promotion of supports with proper elements can increase the catalysts basicity and its poison resistance related to sulfur components. Efforts have focused mostly on the addition of CeO_2 [136–139] and ZrO_2 [140,141] as promoters to alumina supports.

The addition of ceria on Ni-based catalysts supported on alumina improves their activity and stability in the reforming of heavy tar compounds. Due to oxygen vacancies with high mobility, CeO_2 acts as an oxygen donor on the catalyst surface [108], favoring the reaction between CO_2 and C, and thus helping to reduce coke formation promoted by the reverse Boudouard reaction. In the presence of H_2S , the promotion effect of cerium, due to its oxidative properties, enhances the sulfur tolerance of Ni/ Al_2O_3 , thus reducing the poisonous effects of hydrogen sulfide on the Ni active sites [136–139,142].

Similarly, the use of ZrO_2 has shown some resistance to sulfur components; however, the main drawback of ZrO_2 is its low surface area compared to other supports [140,141].

Recently, high and stable catalytic activity of pure CeO_2 in the dry reforming reaction in the presence of 2000 ppm of H_2S was demonstrated by Taira et al. [143]. H_2S improved the reducibility of CeO_2 , since sulfur on CeO_2 can change the oxidation state rapidly, contributing to improved oxygen mobility. The swift changes among the oxidation states of sulfur accelerated the re-oxidation of CeO_2 by CO_2 , which in turn decreased the amount of oxygen vacancies on the CeO_2 surface [143].

Another type of support for the catalyst in the reforming reaction largely investigated are perovskite materials, which could improve sulfur resistance by providing labile lattice oxygen atoms that facilitate the oxidation and removal of sulfur from the catalysts [144,145].

The general formula of perovskites is ABO_3 , where A is a metal with a larger ionic radius, typically from the rare-earth group, and B is a metal with a smaller radius, usually from the transition metals group. Partial substitution of A, B, or both allows for the synthesis of a wide variety of compositions with different properties.

Dinka et al. [146] have proved that complex perovskite (ABO_3)-based catalysts can be very effective for the ATR of heavy hydrocarbons. Specifically, it was demonstrated that for LaFeO_3 basic composition, a partial substitution of La by Ce on the A-side enhances the catalyst ability for carbon removal, while corresponding B(Fe)-site substitution by Ni leads to an increase in its catalytic activity. Furthermore, a small amount of metal additives can increase the stability of perovskite-based catalysts in a sulfur-containing environment. For example, it was found that 2 wt% of potassium or 1 wt% of ruthenium substituted on the B-side of the $\text{La}_{0.6}\text{Ce}_{0.4}\text{Fe}_{0.68-\gamma}\text{Ni}_{\gamma}\text{O}_{3-\delta}$ significantly increases its durability during the ATR of a fuel-containing sulfur [146].

For the perovskite catalysts in the family of compositions based on LaMO_3 (where $M = \text{Cr, Mn, Fe, Ni, Co}$), Cr was found to be the best element for B-site doping in terms of maintaining constant H_2 yields, providing some degree of sulfur tolerance when reforming sulfur-containing fuels [147].

A study of the catalytic reforming of a tar model compound over $\text{La}_{1-x}\text{Sr}_x\text{Co}_{0.5}\text{Ti}_{0.5}\text{O}_{3-\delta}$ dual perovskite catalysts highlights the resistance to sulfide upon introduction of 50 ppm of H_2S at 800 $^{\circ}\text{C}$, despite the fact that the conversion on material drops to 20%, which was maintained for 5 h of H_2S exposure. Subsequently, after stopping H_2S in the feed, the catalyst was able to regenerate about 95% of the initial activity at the same reaction temperature [148].

Recently, Wang et al. have reviewed the state-of-art of sulfur poisoning for the perovskite cathode materials of the SOFCs, clarifying the plausible sulfur poisoning mechanism and the relationship between features of chemical reactions and cathode performance

degradation in terms of the effects of electrochemical aspects on the chemical reaction. They found some interesting differences in sulfur poisoning between (La, Sr)CoO_{3-δ} (LSC) and (La, Sr)(Co, Fe)O_{3-δ} (LSCF), which can be correlated with differences in the availability of the adsorption of oxygen molecules on the perovskite oxide surface [149].

5. Concluding Remarks

The sulfur tolerance of reforming catalysts always represents a severe issue in determining the performance and stability in the reaction process, which is particularly relevant for biofuels. Several studies and reviews have been published on this topic, and various approaches have been investigated in the last decade to increase the resistance to sulfur in heterogeneous catalysts, including an incorporation of different elements; a modification of the physico-chemical structure, e.g., core-shell morphology; a modification of electronic properties; alloying; synthesis procedures; and process experimental conditions. Far from being exhaustive, the present work aims at condensing the most relevant information present in the literature to design possible catalyst architectures for sulfur-resistant materials.

Different challenges remain to be solved by researchers: i) the evaluation of the sulfur adsorption capacity of reforming catalysts in order to measure the resistance to poisoning and to avoid the blocks of the active catalytic sites, ii) the investigation of the catalytic stability of a reforming catalyst in the simultaneous presence of different types of deactivating compounds (H₂S, higher hydrocarbons, and siloxane compounds), and iii) the evaluation of reforming options to increase the catalyst lifetime and/or reduce the poisoning effect of sulfur compounds.

Author Contributions: All authors contributed to writing the paper. All authors have read and agreed to the published version of the manuscript.

Funding: This publication was supported by Direct Utilization of Bio-Fuels in Solid Oxide Fuel Cells for Sustainable and Decentralized Production of Electric Power and Heat Project (Directbiopower, Grant Number 2017FCFYHK) and funded by the Ministry of University and Research-Italy.

Conflicts of Interest: The authors declare no conflict of interest.

References

1. Bogdanov, D.; Ram, M.; Aghahosseini, A.; Gulagi, A.; Oyewo, A.S.; Child, M.; Caldera, U.; Sadovskaia, K.; Farfan, J.; De Souza Noel Simas Barbosa, L.; et al. Low-cost renewable electricity as the key driver of the global energy transition towards sustainability. *Energy* **2021**, *227*, 120467. [CrossRef]
2. Bonaccorsi, L.; Fotia, A.; Malara, A.; Frontera, P. Advanced adsorbent materials for waste energy recovery. *Energies* **2020**, *13*, 4299. [CrossRef]
3. Freni, A.; Calabrese, L.; Malara, A.; Frontera, P.; Bonaccorsi, L. Silica gel microfibres by electrospinning for adsorption chillers. *Energy* **2019**, *187*, 115971. [CrossRef]
4. Frontera, P.; Kumita, M.; Malara, A.; Nishizawa, J.; Bonaccorsi, L. Manufacturing and assessment of electrospun PVP/TEOS microfibres for adsorptive heat transformers. *Coatings* **2019**, *9*, 443. [CrossRef]
5. IEA 2020, World Energy Outlook 2020, IEA, Paris. Available online: <https://www.iea.org/reports/world-energy-outlook-2020> (accessed on 31 July 2021).
6. IEA. *Energy and Industrial Process CO₂ Emissions and Reduction Levers in WEO 2020 Scenarios, 2015–2030*; IEA: Paris, France, 2020.
7. Nikolaidis, P.; Poullikkas, A. A comparative overview of hydrogen production processes. *Renew. Sustain. Energy Rev.* **2017**, *67*, 597–611. [CrossRef]
8. Momirlan, M.; Veziroglu, T.N. Current status of hydrogen energy. *Renew. Sustain. Energy Rev.* **2002**, *6*, 141–179. [CrossRef]
9. Pasman, H.J.; Rogers, W.J. Safety challenges in view of the upcoming hydrogen economy: An overview. *J. Loss Prev. Process Ind.* **2010**, *23*, 697–704. [CrossRef]
10. Kapdan, I.K.; Kargi, F. Bio-hydrogen production from waste materials. *Enzym. Microb. Technol.* **2006**, *38*, 569–582. [CrossRef]
11. Balat, H.; Kırtay, E. Hydrogen from biomass—Present scenario and future prospects. *Int. J. Hydrogen Energy* **2010**, *35*, 7416–7426. [CrossRef]
12. Levin, D.B.; Chahine, R. Challenges for renewable hydrogen production from biomass. *Int. J. Hydrogen Energy* **2010**, *35*, 4962–4969. [CrossRef]
13. Candamano, S.; Frontera, P.; Macario, A.; Aloise, A.; Crea, F. New material as Ni-support for hydrogen production by ethanol conversion. *WIT Trans. Eng. Sci.* **2014**, *2014*, 115–122.

14. Eni for 2020 Carbon Neutrality by 2050. Available online: <https://www.eni.com/assets/documents/ita/sostenibilita/2020/Eni-for-2020-neutralita-carbonica-al-2050.pdf> (accessed on 31 July 2021).
15. Profeti, L.P.R.; Ticianelli, E.A.; Assaf, E.M. Production of hydrogen via steam reforming of biofuels on Ni/CeO₂-Al₂O₃ catalysts promoted by noble metals. *Int. J. Hydrogen Energy* **2009**, *34*, 5049–5060. [[CrossRef](#)]
16. Nahar, G.; Dupont, V.; Twigg, M.V.; Dvininov, E. Feasibility of hydrogen production from steam reforming of biodiesel (FAME) feedstock on Ni-supported catalysts. *Appl. Catal. B Environ.* **2015**, *168*, 228–242. [[CrossRef](#)]
17. Dou, B.; Song, Y.; Wang, C.; Chen, H.; Xu, Y. Hydrogen production from catalytic steam reforming of biodiesel byproduct glycerol: Issues and challenges. *Renew. Sustain. Energy Rev.* **2014**, *30*, 950–960. [[CrossRef](#)]
18. Veiga, S.; Faccio, R.; Romero, M.; Bussi, J. Utilization of waste crude glycerol for hydrogen production via steam reforming over Ni-La-Zr catalysts. *Biomass Bioenergy* **2020**, *135*, 105508. [[CrossRef](#)]
19. Martin, S.; Wörner, A. On-board reforming of biodiesel and bioethanol for high temperature PEM fuel cells: Comparison of autothermal reforming and steam reforming. *J. Power Source* **2011**, *196*, 3163–3171. [[CrossRef](#)]
20. Nahar, G.A. Hydrogen rich gas production by the autothermal reforming of biodiesel (FAME) for utilization in the solid-oxide fuel cells: A thermodynamic analysis. *Int. J. Hydrogen Energy* **2010**, *35*, 8891–8911. [[CrossRef](#)]
21. Tripodi, A.; Compagnoni, M.; Bahadori, E.; Rossetti, I.; Ramis, G. Process intensification by exploiting diluted 2nd generation bio-ethanol in the low-temperature steam reforming process. *Top. Catal.* **2018**, *61*, 1832–1841. [[CrossRef](#)]
22. Malara, A.; Frontera, P.; Antonucci, P.; Macario, A. Smart recycling of carbon oxides: Current status of methanation reaction. *Curr. Opin. Green Sustain. Chem.* **2020**, *26*, 100376. [[CrossRef](#)]
23. Frontera, P.; Macario, A.; Malara, A.; Santangelo, S.; Triolo, C.; Crea, F.; Antonucci, P. Trimetallic ni-based catalysts over gadolinia-doped ceria for green fuel production. *Catalysts* **2018**, *8*, 435. [[CrossRef](#)]
24. Jamsak, W.; Assabumrungrat, S.; Douglas, P.L.; Laosiripojana, N.; Charojrochkul, S. Theoretical performance analysis of ethanol-fuelled solid oxide fuel cells with different electrolytes. *Chem. Eng. J.* **2006**, *119*, 11–18. [[CrossRef](#)]
25. Colmenares, J.C.; Colmenares Quintero, R.F.; Pieta, I.S. Catalytic dry reforming for biomass-based fuels processing: Progress and future perspectives. *Energy Technol.* **2016**, *4*, 881–890. [[CrossRef](#)]
26. Macario, A.; Frontera, P.; Candamano, S.; Crea, F.; Luca, P.D.; Antonucci, P.L. Nanostructured catalysts for dry-reforming of methane. *J. Nanosci. Nanotechnol.* **2019**, *19*, 3135–3147. [[CrossRef](#)]
27. Song, Y.; Ozdemir, E.; Ramesh, S.; Adishev, A.; Subramanian, S.; Harale, A.; Albuali, M.; Fadhel, B.A.; Jamal, A.; Moon, D. Dry reforming of methane by stable Ni-Mo nanocatalysts on single-crystalline MgO. *Science* **2020**, *367*, 777–781. [[CrossRef](#)]
28. Cheekatamarla, P.K.; Finnerty, C.M. Reforming catalysts for hydrogen generation in fuel cell applications. *J. Power Source* **2006**, *160*, 490–499. [[CrossRef](#)]
29. Ni, M.; Leung, D.Y.C.; Leung, M.K.H. A review on reforming bio-ethanol for hydrogen production. *Int. J. Hydrogen Energy* **2007**, *32*, 3238–3247. [[CrossRef](#)]
30. Dhanala, V.; Maity, S.K.; Shee, D. Roles of supports (γ -Al₂O₃, SiO₂, ZrO₂) and performance of metals (Ni, Co, Mo) in steam reforming of isobutanol. *RSC Adv.* **2015**, *5*, 52522–52532. [[CrossRef](#)]
31. Frontera, P.; Macario, A.; Aloise, A.; Crea, F.; Antonucci, P.L.; Nagy, J.B.; Frusteri, F.; Giordano, G. Catalytic dry-reforming on Ni-zeolite supported catalyst. *Catal. Today* **2012**, *179*, 52–60. [[CrossRef](#)]
32. Pawelec, B.; Damyanova, S.; Arishtirova, K.; Fierro, J.L.G.; Petrov, L. Structural and surface features of PtNi catalysts for reforming of methane with CO₂. *Appl. Catal. A Gen.* **2007**, *323*, 188–201. [[CrossRef](#)]
33. Srisriwat, N.; Therdthianwong, S.; Therdthianwong, A. Oxidative steam reforming of ethanol over Ni/Al₂O₃ catalysts promoted by CeO₂, ZrO₂ and CeO₂-ZrO₂. *Int. J. Hydrogen Energy* **2009**, *34*, 2224–2234. [[CrossRef](#)]
34. Frontera, P.; Macario, A.; Candamano, S.; Crea, F.; Barberio, M.; Antonucci, P.L. Alkaline-promoted zeolites for methane dry-reforming catalyst preparation. *Adv. Sci. Lett.* **2017**, *23*, 5883–5885. [[CrossRef](#)]
35. Zhang, B.; Tang, X.; Li, Y.; Xu, Y.; Shen, W. Hydrogen production from steam reforming of ethanol and glycerol over ceria-supported metal catalysts. *Int. J. Hydrogen Energy* **2007**, *32*, 2367–2373. [[CrossRef](#)]
36. Bellido, J.D.A.; Assaf, E.M. Nickel catalysts supported on ZrO₂, Y₂O₃-stabilized ZrO₂ and CaO-stabilized ZrO₂ for the steam reforming of ethanol: Effect of the support and nickel load. *J. Power Source* **2008**, *177*, 24–32. [[CrossRef](#)]
37. Frontera, P.; Macario, A.; Aloise, A.; Antonucci, P.L.; Giordano, G.; Nagy, J.B. Effect of support surface on methane dry-reforming catalyst preparation. *Catal. Today* **2013**, *218*, 18–29. [[CrossRef](#)]
38. Contreras, J.L.; Salmones, J.; Colín-Luna, J.A.; Nuño, L.; Quintana, B.; Córdova, I.; Zeifert, B.; Tapia, C.; Fuentes, G.A. Catalysts for H₂ production using the ethanol steam reforming (a review). *Int. J. Hydrogen Energy* **2014**, *39*, 18835–18853. [[CrossRef](#)]
39. Fajardo, H.V.; Longo, E.; Mezalira, D.Z.; Nuernberg, G.B.; Almerindo, G.I.; Collasiol, A.; Probst, L.F.D.; Garcia, I.T.S.; Carreño, N.L. V Influence of support on catalytic behavior of nickel catalysts in the steam reforming of ethanol for hydrogen production. *Environ. Chem. Lett.* **2010**, *8*, 79–85. [[CrossRef](#)]
40. Frontera, P.; Aloise, A.; Macario, A.; Antonucci, P.L.; Crea, F.; Giordano, G.; Nagy, J.B. Bimetallic zeolite catalyst for CO₂ reforming of methane. *Top. Catal.* **2010**, *53*, 265–272. [[CrossRef](#)]
41. Miceli, M.; Frontera, P.; Macario, A.; Malara, A. Recovery/Reuse of Heterogeneous Supported Spent Catalysts. *Catalysts* **2021**, *11*, 591. [[CrossRef](#)]
42. Wang, L.; Murata, K.; Inaba, M. Development of novel highly active and sulphur-tolerant catalysts for steam reforming of liquid hydrocarbons to produce hydrogen. *Appl. Catal. A Gen.* **2004**, *257*, 43–47. [[CrossRef](#)]

43. Zhang, J.; Wang, Y.; Ma, R.; Wu, D. Characterization of alumina-supported Ni and Ni-Pd catalysts for partial oxidation and steam reforming of hydrocarbons. *Appl. Catal. A Gen.* **2003**, *243*, 251–259. [CrossRef]
44. Trimm, D.L.; Adesina, A.A.; Cant, N.W. The conversion of gasoline to hydrogen for on-board vehicle applications. *Catal. today* **2004**, *93*, 17–22. [CrossRef]
45. Resini, C.; Delgado, M.C.H.; Presto, S.; Alemany, L.J.; Riani, P.; Marazza, R.; Ramis, G.; Busca, G. Ytria-stabilized zirconia (YSZ) supported Ni-Co alloys (precursor of SOFC anodes) as catalysts for the steam reforming of ethanol. *Int. J. Hydrogen Energy* **2008**, *33*, 3728–3735. [CrossRef]
46. Yeo, T.Y.; Ashok, J.; Kawi, S. Recent developments in sulphur-resilient catalytic systems for syngas production. *Renew. Sustain. Energy Rev.* **2019**, *100*, 52–70. [CrossRef]
47. Young, C.G.; Amais, R.S.; Schiavo, D.; Garcia, E.E.; Nóbrega, J.A.; Jones, B.T. Determination of sulfur in biodiesel microemulsions using the summation of the intensities of multiple emission lines. *Talanta* **2011**, *84*, 995–999. [CrossRef]
48. Amais, R.S.; Long, S.E.; Nóbrega, J.A.; Christopher, S.J. Determination of trace sulfur in biodiesel and diesel standard reference materials by isotope dilution sector field inductively coupled plasma mass spectrometry. *Anal. Chim. Acta* **2014**, *806*, 91–96. [CrossRef]
49. Dannesboe, C.; Hansen, J.B.; Johannsen, I. Removal of sulfur contaminants from biogas to enable direct catalytic methanation. *Biomass Convers. Biorefinery* **2019**, 1–12. [CrossRef]
50. Song, C.; Ma, X. New design approaches to ultra-clean diesel fuels by deep desulfurization and deep dearomatization. *Appl. Catal. B Environ.* **2003**, *41*, 207–238. [CrossRef]
51. Bartholomew, C.H.; Weatherbee, G.D.; Jarvi, G.A. Sulfur poisoning of nickel methanation catalysts: I. in situ deactivation by H₂S of nickel and nickel bimetallics. *J. Catal.* **1979**, *60*, 257–269. [CrossRef]
52. Bartholomew, C.H. Mechanisms of catalyst deactivation. *Appl. Catal. A Gen.* **2001**, *212*, 17–60. [CrossRef]
53. Froment, G.F.; Delmon, B. *Catalyst Deactivation 1987*; Elsevier: Amsterdam, The Netherlands, 1987; ISBN 0080960685.
54. Bartholomew, C.H.; Agrawal, P.K.; Katzer, J.R. Sulfur poisoning of metals. *Adv. Catal.* **1982**, *31*, 135–242.
55. Grossmann, A.; Erley, W.; Ibach, H. Adsorbate-induced surface stress and surface reconstruction: Oxygen, sulfur and carbon on Ni(111). *Surf. Sci.* **1995**, *337*, 183–189. [CrossRef]
56. Ruan, L.; Stensgaard, I.; Besenbacher, F.; Laegsgaard, E. Observation of a missing-row structure on an fcc (111) surface: The (5√3 × 2) S phase on Ni (111) studied by scanning tunneling microscopy. *Phys. Rev. Lett.* **1993**, *71*, 2963. [CrossRef] [PubMed]
57. Argyle, M.D.; Bartholomew, C.H. Heterogeneous Catalyst Deactivation and Regeneration: A Review. *Catalysts* **2015**, *5*, 145–269. [CrossRef]
58. Beale, A.M.; Gibson, E.K.; O'Brien, M.G.; Jacques, S.D.M.; Cernik, R.J.; Di Michiel, M.; Cobden, P.D.; Pirgon-Galin, Ö.; van de Water, L.; Watson, M.J. Chemical imaging of the sulfur-induced deactivation of Cu/ZnO catalyst bodies. *J. Catal.* **2014**, *314*, 94–100. [CrossRef]
59. Wilburn, M.S.; Epling, W.S. Sulfur deactivation and regeneration of mono-and bimetallic Pd-Pt methane oxidation catalysts. *Appl. Catal. B Environ.* **2017**, *206*, 589–598. [CrossRef]
60. Luo, J.Y.; Kisinger, D.; Abedi, A.; Epling, W.S. Sulfur release from a model Pt/Al₂O₃ diesel oxidation catalyst: Temperature-programmed and step-response techniques characterization. *Appl. Catal. A Gen.* **2010**, *383*, 182–191. [CrossRef]
61. Wilburn, M.S.; Epling, W.S. Formation and decomposition of sulfite and sulfate species on Pt/Pd catalysts: An SO₂ oxidation and sulfur exposure study. *ACS Catal.* **2018**, *9*, 640–648. [CrossRef]
62. Ali Khan, M.H.; Daiyan, R.; Neal, P.; Haque, N.; MacGill, I.; Amal, R. A framework for assessing economics of blue hydrogen production from steam methane reforming using carbon capture storage & utilisation. *Int. J. Hydrogen Energy* **2021**, *46*, 22685–22706. [CrossRef]
63. Sadykov, V.; Mezentseva, N.; Fedorova, Y.; Lukashevich, A.; Pelipenko, V.; Kuzmin, V.; Simonov, M.; Ishchenko, A.; Vostrikov, Z.; Bobrova, L.; et al. Structured catalysts for steam/ autothermal reforming of biofuels on heat-conducting substrates: Design and performance. *Catal. Today* **2015**, *251*, 19–27. [CrossRef]
64. Iulianelli, A.; Dalena, F.; Basile, A. H₂ production from bioalcohols and biomethane steam reforming in membrane reactors. In *Bioenergy Systems for the Future*; Dalena, F., Basile, A., Rossi, C.B.T., Eds.; Woodhead Publishing: Sawston, UK, 2017; pp. 321–344. ISBN 978-0-08-101031-0.
65. Shah, Y.T.; Gardner, T.H. Dry reforming of hydrocarbon feedstocks. *Catal. Rev.* **2014**, *56*, 476–536. [CrossRef]
66. Jung, S.; Lee, J.; Moon, D.H.; Kim, K.-H.; Kwon, E.E. Upgrading biogas into syngas through dry reforming. *Renew. Sustain. Energy Rev.* **2021**, *143*, 110949. [CrossRef]
67. Gao, Y.; Golmakani, A.; Nabavi, S.A.; Jiang, J.; Manovic, V. Simulative optimization of catalyst configuration for biogas dry reforming. *Int. J. Hydrogen Energy* **2021**, *46*, 12835–12845. [CrossRef]
68. Pecate, S.; Kessas, S.A.; Morin, M.; Hemati, M. Beech wood gasification in a dense and fast internally circulating fluidized bed. *Fuel* **2019**, *236*, 554–573. [CrossRef]
69. García, L.; Salvador, M.L.; Arauzo, J.; Bilbao, R. Catalytic Steam Gasification of Pine Sawdust. Effect of Catalyst Weight/Biomass Flow Rate and Steam/Biomass Ratios on Gas Production and Composition. *Energy Fuels* **1999**, *13*, 851–859. [CrossRef]
70. ISO 16994:2016(en)Solid Biofuels—Determination of Total Content of Sulfur and Chlorine. Available online: <https://www.iso.org/standard/70097.html> (accessed on 31 July 2021).
71. Demirbas, A. Biofuels securing the planet's future energy needs. *Energy Convers. Manag.* **2009**, *50*, 2239–2249. [CrossRef]

72. Susmozas, A.; Martín-Sampedro, R.; Ibarra, D.; Eugenio, M.E.; Iglesias, R.; Manzanares, P.; Moreno, A.D. Process Strategies for the Transition of 1G to Advanced Bioethanol Production. *Processes* **2020**, *8*, 1310. [CrossRef]
73. Hartmann, H. Solid biofuels, fuels and their characteristics. In *Encyclopedia of Sustainability Science and Technology*; Springer: New York, NY, USA, 2012. [CrossRef]
74. Obernberger, I.; Brunner, T.; Bärnthaler, G. Chemical properties of solid biofuels—Significance and impact. *Biomass Bioenergy* **2006**, *30*, 973–982. [CrossRef]
75. He, B.B.; Van Gerpen, J.H.; Thompson, J.C. Sulfur content in selected oils and fats and their corresponding methyl esters. *Appl. Eng. Agric.* **2009**, *25*, 223–226.
76. Sajjadi, B.; Raman, A.A.A.; Arandiyani, H. A comprehensive review on properties of edible and non-edible vegetable oil-based biodiesel: Composition, specifications and prediction models. *Renew. Sustain. Energy Rev.* **2016**, *63*, 62–92. [CrossRef]
77. Rasi, S.; Veijanen, A.; Rintala, J. Trace compounds of biogas from different biogas production plants. *Energy* **2007**, *32*, 1375–1380. [CrossRef]
78. Li, Y.; Alaimo, C.P.; Kim, M.; Kado, N.Y.; Peppers, J.; Xue, J.; Wan, C.; Green, P.G.; Zhang, R.; Jenkins, B.M. Composition and toxicity of biogas produced from different feedstocks in California. *Environ. Sci. Technol.* **2019**, *53*, 11569–11579. [CrossRef]
79. Global Biofuel Production in 2019 and Forecast to 2025—IEA. Available online: <https://www.iea.org/data-and-statistics/charts/global-biofuel-production-in-2019-and-forecast-to-2025> (accessed on 31 July 2021).
80. Nelson, A.E. *Fundamentals of Industrial Catalytic Processes*, 2nd ed.; Bartholomew, C.H., Farrauto, R.J., Eds.; John Wiley and Sons: Hoboken, NJ, USA, 2006. [CrossRef]
81. Sanchez, N.; Ruiz, R.; Hacker, V.; Cobo, M. Impact of bioethanol impurities on steam reforming for hydrogen production: A review. *Int. J. Hydrogen Energy* **2020**, *45*, 11923–11942. [CrossRef]
82. Yamazaki, T.; Kikuchi, N.; Katoh, M.; Hirose, T.; Saito, H.; Yoshikawa, T.; Wada, M. Behavior of steam reforming reaction for bio-ethanol over Pt/ZrO₂ catalysts. *Appl. Catal. B Environ.* **2010**, *99*, 81–88. [CrossRef]
83. McPhee, W.A.G.; Boucher, M.; Stuart, J.; Parnas, R.S.; Koslowski, M.; Tao, T.; Wilhite, B.A. Demonstration of a liquid-tin anode solid-oxide fuel cell (LTA-SOFC) operating from biodiesel fuel. *Energy Fuels* **2009**, *23*, 5036–5041. [CrossRef]
84. Nahar, G.; Kendall, K. Biodiesel formulations as fuel for internally reforming solid oxide fuel cell. *Fuel Process. Technol.* **2011**, *92*, 1345–1354. [CrossRef]
85. Na Rungsi, A.; Truong, T.H.; Thunyaratchatanon, C.; Luengnaruemitchai, A.; Chollacoop, N.; Chen, S.-Y.; Mochizuki, T.; Takagi, H.; Yoshimura, Y. Tuning the porosity of sulfur-resistant Pd-Pt/MCM-41 bimetallic catalysts for partial hydrogenation of soybean oil-derived biodiesel. *Fuel* **2021**, *298*, 120658. [CrossRef]
86. Ma, H.; Addy, M.M.; Anderson, E.; Liu, W.; Liu, Y.; Nie, Y.; Chen, P.; Cheng, B.; Lei, H.; Ruan, R. A novel process for low-sulfur biodiesel production from scum waste. *Bioresour. Technol.* **2016**, *214*, 826–835. [CrossRef]
87. Biodiesel Fuel Testing Europe EN-14214. Available online: <https://www.intertek.com/biofuels/biodiesel/en-14214/>, (accessed on 31 July 2021).
88. ASTM D6751-20a Standard Specification for Biodiesel Fuel Blend Stock (B100) for Middle Distillate Fuels. Available online: <https://standards.globalspec.com/std/14334223/astm-d6751-20a>, (accessed on 31 July 2021).
89. Elghawi, U.; Theinnoi, K.; Sitshebo, S.; Tsolakis, A.; Wyszynski, M.L.; Xu, H.M.; Cracknell, R.F.; Clark, R.H.; Mayouf, A. GC-MS determination of low hydrocarbon species (C1–C6) from a diesel partial oxidation reformer. *Int. J. Hydrogen Energy* **2008**, *33*, 7074–7083. [CrossRef]
90. Kraaij, G.J.; Specchia, S.; Bollito, G.; Mutri, L.; Wails, D. Biodiesel fuel processor for APU applications. *Int. J. Hydrogen Energy* **2009**, *34*, 4495–4499. [CrossRef]
91. Lin, J.; Trabold, T.A.; Walluk, M.R.; Smith, D.F. Bio-fuel reformation for solid oxide fuel cell applications. Part 3: Biodiesel–diesel blends. *Int. J. Hydrogen Energy* **2014**, *39*, 196–208. [CrossRef]
92. Zhao, X.; Joseph, B.; Kuhn, J.; Ozcan, S. Biogas reforming to syngas: A review. *Science* **2020**, *23*, 101082. [CrossRef] [PubMed]
93. Vita, A.; Italiano, C.; Fabiano, C.; Laganà, M.; Pino, L. Influence of Ce-precursor and fuel on structure and catalytic activity of combustion synthesized Ni/CeO₂ catalysts for biogas oxidative steam reforming. *Mater. Chem. Phys.* **2015**, *163*, 337–347. [CrossRef]
94. Bi, S.; Qiao, W.; Xiong, L.; Ricci, M.; Adani, F.; Dong, R. Effects of organic loading rate on anaerobic digestion of chicken manure under mesophilic and thermophilic conditions. *Renew. Energy* **2019**, *139*, 242–250. [CrossRef]
95. Ruan, R.; Zhang, Y.; Chen, P.; Liu, S.; Fan, L.; Zhou, N.; Ding, K.; Peng, P.; Addy, M.; Cheng, Y.; et al. Biofuels: Introduction. In *Biofuels: Alternative Feedstocks and Conversion Processes for the Production of Liquid and Gaseous Biofuels*; Academic Press: Cambridge, MA, USA, 2019; pp. 3–43.
96. Chandra, R.; Takeuchi, H.; Hasegawa, T. Methane production from lignocellulosic agricultural crop wastes: A review in context to second generation of biofuel production. *Renew. Sustain. Energy Rev.* **2012**, *16*, 1462–1476. [CrossRef]
97. Wachter, P.; Gaber, C.; Raic, J.; Demuth, M.; Hochenauer, C. Experimental investigation on H₂S and SO₂ sulphur poisoning and regeneration of a commercially available Ni-catalyst during methane tri-reforming. *Int. J. Hydrogen Energy* **2021**, *46*, 3437–3452. [CrossRef]
98. Mohamed, D.K.B.; Veksha, A.; Lim, T.T.; Lisak, G. Highly active and poison-tolerant nickel catalysts for tar reforming synthesized through controlled hydrothermal synthesis. *Appl. Catal. A Gen.* **2020**, *607*, 117779. [CrossRef]

99. Jiang, C.; Loisel, E.; Cullen, D.A.; Dorman, J.A.; Dooley, K.M. On the enhanced sulfur and coking tolerance of Ni-Co-rare earth oxide catalysts for the dry reforming of methane. *J. Catal.* **2021**, *393*, 215–229. [[CrossRef](#)]
100. Escudero, M.J.; Maffiotte, C.A.; Serrano, J.L. Long-term operation of a solid oxide fuel cell with MoNi–CeO₂ as anode directly fed by biogas containing simultaneously sulphur and siloxane. *J. Power Source* **2021**, *481*, 229048. [[CrossRef](#)]
101. Gao, K.; Sahraei, O.A.; Iliuta, M.C. Development of residue coal fly ash supported nickel catalyst for H₂ production via glycerol steam reforming. *Appl. Catal. B Environ.* **2021**, *291*, 119958. [[CrossRef](#)]
102. Iulianelli, A.; Manisco, M.; Bion, N.; Le Valant, A.; Epron, F.; Colpan, C.O.; Esposito, E.; Jansen, J.C.; Gensini, M.; Caravella, A. Sustainable H₂ generation via steam reforming of biogas in membrane reactors: H₂S effects on membrane performance and catalytic activity. *Int. J. Hydrogen Energy* **2020**, *46*, 29183–29197. [[CrossRef](#)]
103. Yin, W.; Guilhaume, N.; Schuurman, Y. Model biogas reforming over Ni-Rh/MgAl₂O₄ catalyst. Effect of gas impurities. *Chem. Eng. J.* **2020**, *398*, 125534. [[CrossRef](#)]
104. Ashok, J.; Das, S.; Dewangan, N.; Kawi, S. Steam reforming of surrogate diesel model over hydrotalcite-derived MO–CaO–Al₂O₃ (M = Ni & Co) catalysts for SOFC applications. *Fuel* **2021**, *291*, 120194.
105. Liu, X.; Yan, J.; Mao, J.; He, D.; Yang, S.; Mei, Y.; Luo, Y. Inhibitor, co-catalyst, or intermetallic promoter? Probing the sulfur-tolerance of MoO_x surface decoration on Ni/SiO₂ during methane dry reforming. *Appl. Surf. Sci.* **2021**, *548*, 149231. [[CrossRef](#)]
106. Suslick, K.S.; Skrabalak, S.E. *Handbook of Heterogeneous Catalysis*; Ertl, G., Knozinger, H., Weitkamp, J., Eds.; Wiley-VCH: Weinheim, Germany, 1997; Volume 3, pp. 1350–1357.
107. Frontera, P.; Malara, A.; Modafferi, V.; Antonucci, V.; Antonucci, P.; Macario, A. Catalytic activity of Ni-Co supported metals in carbon dioxides methanation. *Can. J. Chem. Eng.* **2020**, *98*, 1924–1934. [[CrossRef](#)]
108. Frontera, P.; Macario, A.; Malara, A.; Antonucci, V.; Modafferi, V.; Antonucci, P.L. Simultaneous methanation of carbon oxides on nickel-iron catalysts supported on ceria-doped gadolinia. *Catal. Today* **2020**, *357*, 565–572. [[CrossRef](#)]
109. Frontera, P.; Macario, A.; Malara, A.; Modafferi, V.; Mascolo, M.C.; Candamano, S.; Crea, F.; Antonucci, P. CO₂ and CO hydrogenation over Ni-supported materials. *Funct. Mater. Lett.* **2018**, *11*, 1850061. [[CrossRef](#)]
110. Candamano, S.; Frontera, P.; Macario, A.; Crea, F.; Nagy, J.B.; Antonucci, P.L. Preparation and characterization of active Ni-supported catalyst for syngas production. *Chem. Eng. Res. Des.* **2015**, *96*, 78–86. [[CrossRef](#)]
111. Sehested, J. Four challenges for nickel steam-reforming catalysts. *Catal. Today* **2006**, *111*, 103–110. [[CrossRef](#)]
112. Jablonski, W.S.; Villano, S.M.; Dean, A.M. A comparison of H₂S, SO₂, and COS poisoning on Ni/YSZ and Ni/K₂O–CaAl₂O₄ during methane steam and dry reforming. *Appl. Catal. A Gen.* **2015**, *502*, 399–409. [[CrossRef](#)]
113. Zaza, F.; Paoletti, C.; LoPresti, R.; Simonetti, E.; Pasquali, M. Studies on sulfur poisoning and development of advanced anodic materials for waste-to-energy fuel cells applications. *J. Power Source* **2010**, *195*, 4043–4050. [[CrossRef](#)]
114. Di Giulio, N.; Audasso, E.; Bosio, B.; Han, J.; McPhail, S.J. Experimental influence of operating variables on the performances of MCFCs under SO₂ poisoning. *Int. J. Hydrogen Energy* **2015**, *40*, 6430–6439. [[CrossRef](#)]
115. Kawase, M.; Mugikura, Y.; Watanabe, T. The effects of H₂S on electrolyte distribution and cell performance in the molten carbonate fuel cell. *J. Electrochem. Soc.* **2000**, *147*, 1240. [[CrossRef](#)]
116. Watanabe, T.; Izaki, Y.; Mugikura, Y.; Morita, H.; Yoshikawa, M.; Kawase, M.; Yoshida, F.; Asano, K. Applicability of molten carbonate fuel cells to various fuels. *J. Power Source* **2006**, *160*, 868–871. [[CrossRef](#)]
117. Hagen, A.; Johnson, G.B.; Hjalmarsson, P. Electrochemical evaluation of sulfur poisoning in a methane-fuelled solid oxide fuel cell: Effect of current density and sulfur concentration. *J. Power Source* **2014**, *272*, 776–785. [[CrossRef](#)]
118. Rodriguez, J.A.; Hrbek, J. Interaction of Sulfur with Well-Defined Metal and Oxide Surfaces: Unraveling the Mysteries behind Catalyst Poisoning and Desulfurization. *Acc. Chem. Res.* **1999**, *32*, 719–728. [[CrossRef](#)]
119. Grgicak, C.M.; Pakulska, M.M.; O'Brien, J.S.; Giorgi, J.B. Synergistic effects of Ni_{1–xCox}-YSZ and Ni_{1–xCu}-YSZ alloyed cermet SOFC anodes for oxidation of hydrogen and methane fuels containing H₂S. *J. Power Source* **2008**, *183*, 26–33. [[CrossRef](#)]
120. O'Brien, J.S.; Giorgi, J.B. Carbon and Sulfur Poisoning in SOFC Anodes: Ni_{0.7}Co_{0.3}-YSZ Performance with Hydrocarbons, Alcohols and Biodiesel Fuels Containing H₂S. *ECS Trans.* **2010**, *28*, 221. [[CrossRef](#)]
121. Saha, B.; Khan, A.; Ibrahim, H.; Idem, R. Evaluating the performance of non-precious metal based catalysts for sulfur-tolerance during the dry reforming of biogas. *Fuel* **2014**, *120*, 202–217. [[CrossRef](#)]
122. Gaillard, M.; Virginie, M.; Khodakov, A.Y. New molybdenum-based catalysts for dry reforming of methane in presence of sulfur: A promising way for biogas valorization. *Catal. Today* **2017**, *289*, 143–150. [[CrossRef](#)]
123. Quincoces, C.E.; de Vargas, S.P.; Grange, P.; González, M.G. Role of Mo in CO₂ reforming of CH₄ over Mo promoted Ni/Al₂O₃ catalysts. *Mater. Lett.* **2002**, *56*, 698–704. [[CrossRef](#)]
124. Strohm, J.J.; Zheng, J.; Song, C. Low-temperature steam reforming of jet fuel in the absence and presence of sulfur over Rh and Rh–Ni catalysts for fuel cells. *J. Catal.* **2006**, *238*, 309–320. [[CrossRef](#)]
125. Kaila, R.K.; Krause, A.O.I. Autothermal reforming of simulated gasoline and diesel fuels. *Int. J. Hydrogen Energy* **2006**, *31*, 1934–1941. [[CrossRef](#)]
126. Irusta, S.; Cornaglia, L.M.; Lombardo, E.A. Hydrogen production using Ni–Rh on ZrO₂ as potential low-temperature catalysts for membrane reactors. *J. Catal.* **2002**, *210*, 263–272. [[CrossRef](#)]
127. Martin, S.; Kraaij, G.; Ascher, T.; Wails, D.; Wörner, A. An experimental investigation of biodiesel steam reforming. *Int. J. Hydrogen Energy* **2015**, *40*, 95–105. [[CrossRef](#)]

128. Xie, C.; Chen, Y.; Li, Y.; Wang, X.; Song, C. Influence of sulfur on the carbon deposition in steam reforming of liquid hydrocarbons over CeO₂-Al₂O₃ supported Ni and Rh catalysts. *Appl. Catal. A Gen.* **2011**, *394*, 32–40. [[CrossRef](#)]
129. Kantserova, M.R.; Orlyk, S.M.; Vasylyev, O.D. Catalytic activity and resistance to sulfur poisoning of nickel-containing composites based on stabilized zirconia in tri-reforming of methane. *Theor. Exp. Chem.* **2018**, *53*, 387–394. [[CrossRef](#)]
130. Zheng, L.L.; Wang, X.; Zhang, L.; Wang, J.-Y.; Jiang, S.P. Effect of Pd-impregnation on performance, sulfur poisoning and tolerance of Ni/GDC anode of solid oxide fuel cells. *Int. J. Hydrogen Energy* **2012**, *37*, 10299–10310. [[CrossRef](#)]
131. Sapountzi, F.M.; Zhao, C.; Boréave, A.; Retailleau-Mevel, L.; Niakolas, D.; Neofytidis, C.; Vernoux, P. Sulphur tolerance of Au-modified Ni/GDC during catalytic methane steam reforming. *Catal. Sci. Technol.* **2018**, *8*, 1578–1588. [[CrossRef](#)]
132. Vesselli, E.; Peressi, M. Nanoscale Control of Metal Clusters on Templating Supports. In *Studies in Surface Science and Catalysis*; Elsevier: Amsterdam, The Netherlands, 2017; Volume 177, pp. 285–315. ISBN 0167-2991.
133. Malara, A.; Paone, E.; Bonaccorsi, L.; Mauriello, F.; Macario, A.; Frontera, P. Pd/Fe₃O₄ nanofibers for the catalytic conversion of lignin-derived benzyl phenyl ether under transfer hydrogenolysis conditions. *Catalysts* **2020**, *10*, 20. [[CrossRef](#)]
134. Satterfield, C.N. *Heterogeneous Catalysis in Industrial Practice*, 2nd ed.; McGraw-Hill: New York, NY, USA, 1991.
135. Twigg, M.V. *Catalyst Handbook*; Routledge, Taylor&Francis Group: London, UK, 2018; ISBN 1315138867.
136. Bereketidou, O.A.; Goula, M.A. Biogas reforming for syngas production over nickel supported on ceria—Alumina catalysts. *Catal. Today* **2012**, *195*, 93–100. [[CrossRef](#)]
137. Alvarez-Galvan, M.C.; Navarro, R.M.; Rosa, F.; Briceño, Y.; Gordillo Alvarez, F.; Fierro, J.L.G. Performance of La,Ce-modified alumina-supported Pt and Ni catalysts for the oxidative reforming of diesel hydrocarbons. *Int. J. Hydrogen Energy* **2008**, *33*, 652–663. [[CrossRef](#)]
138. Wang, S.; Lu, G.Q.M. Role of CeO₂ in Ni/CeO₂-Al₂O₃ catalysts for carbon dioxide reforming of methane. *Appl. Catal. B Environ.* **1998**, *19*, 267–277. [[CrossRef](#)]
139. Savuto, E.; Navarro, R.M.; Mota, N.; Di Carlo, A.; Bocci, E.; Carlini, M.; Fierro, J.L.G. Steam reforming of tar model compounds over Ni/Mayenite catalysts: Effect of Ce addition. *Fuel* **2018**, *224*, 676–686. [[CrossRef](#)]
140. Kaila, R.K.; Gutiérrez, A.; Slioor, R.; Kemell, M.; Leskelä, M.; Krause, A.O.I. Zirconia-supported bimetallic RhPt catalysts: Characterization and testing in autothermal reforming of simulated gasoline. *Appl. Catal. B Environ.* **2008**, *84*, 223–232. [[CrossRef](#)]
141. Souza, M.M.V.M.; Schmal, M. Methane conversion to synthesis gas by partial oxidation and CO₂ reforming over supported platinum catalysts. *Catal. Lett.* **2003**, *91*, 11–17. [[CrossRef](#)]
142. Laycock, C.J.; Staniforth, J.Z.; Ormerod, R.M. Biogas as a fuel for solid oxide fuel cells and synthesis gas production: Effects of ceria-doping and hydrogen sulfide on the performance of nickel-based anode materials. *Dalt. Trans.* **2011**, *40*, 5494–5504. [[CrossRef](#)] [[PubMed](#)]
143. Taira, K.; Sugiyama, T.; Einaga, H.; Nakao, K.; Suzuki, K. Promoting effect of 2000 ppm H₂S on the dry reforming reaction of CH₄ over pure CeO₂, and in situ observation of the behavior of sulfur during the reaction. *J. Catal.* **2020**, *389*, 611–622. [[CrossRef](#)]
144. Gallego, G.S.; Mondragón, F.; Barrault, J.; Tatibouët, J.-M.; Batiot-Dupeyrat, C. CO₂ reforming of CH₄ over La-Ni based perovskite precursors. *Appl. Catal. A Gen.* **2006**, *311*, 164–171. [[CrossRef](#)]
145. Urasaki, K.; Sekine, Y.; Kawabe, S.; Kikuchi, E.; Matsukata, M. Catalytic activities and coking resistance of Ni/perovskites in steam reforming of methane. *Appl. Catal. A Gen.* **2005**, *286*, 23–29. [[CrossRef](#)]
146. Dinka, P.; Mukasyan, A.S. Perovskite catalysts for the auto-reforming of sulfur containing fuels. *J. Power Source* **2007**, *167*, 472–481. [[CrossRef](#)]
147. Mawdsley, J.R.; Krause, T.R. Rare earth-first-row transition metal perovskites as catalysts for the autothermal reforming of hydrocarbon fuels to generate hydrogen. *Appl. Catal. A Gen.* **2008**, *334*, 311–320. [[CrossRef](#)]
148. Jangam, A.; Das, S.; Pati, S.; Kawi, S. Catalytic reforming of tar model compound over La_{1-x}Sr_x-Co_{0.5}Ti_{0.5}O_{3-δ} dual perovskite catalysts: Resistance to sulfide and chloride compounds. *Appl. Catal. A Gen.* **2021**, *613*, 118013. [[CrossRef](#)]
149. Wang, F.; Kishimoto, H.; Ishiyama, T.; Develos-Bagarinao, K.; Yamaji, K.; Horita, T.; Yokokawa, H. A review of sulfur poisoning of solid oxide fuel cell cathode materials for solid oxide fuel cells. *J. Power Source* **2020**, *478*, 228763. [[CrossRef](#)]